Efficacy of Shear Wave Elastography for Evaluating Right Ventricular Myocardial Fibrosis in Monocrotaline-induced Pulmonary Hypertension Rats

Rie Nakayama (MD)[a], Yoichi Takaya (MD)[a,*], Kazufumi Nakamura (MD, FJCC)[a], Megumi Kondo (MSc)[a], Kaoru Kobayashi (MSc)[a], Yuko Ohno (MSc)[b], Naofumi Amioka (MD)[a], Satoshi Akagi (MD)[a], Masashi Yoshida (MD)[a], Toru Miyoshi (MD, FJCC)[a], Hiroshi Ito (MD, FJCC)[a]

[a] Department of Cardiovascular Medicine, Okayama University Graduate School of Medicine, Dentistry and Pharmaceutical Sciences, Okayama, Japan

[b] Kawasaki University of Medical Welfare, Okayama, Japan

Keywords: Shear wave elastography; Elasticity; Dispersion; Myocardium; Right ventricular function

*Corresponding author: Yoichi Takaya, MD

Department of Cardiovascular Medicine, Okayama University Graduate School of Medicine,

Dentistry and Pharmaceutical Sciences, 2-5-1 Shikata-cho, Kita-ku, Okayama 700-8558, Japan

Tel: +81-86-235-7351

Fax: +81-86-235-7353

E-mail: takayayoichi@okayama-u.ac.jp

Abstract

Background: Right ventricular (RV) function is important for outcomes in pulmonary hypertension. Evaluation of RV myocardial characteristics is useful to assess the disease severity. Shear wave elastography (SWE) provides information of shear wave (SW) elasticity, which is related to tissue hardness, and SW dispersion slope, which reflects tissue viscosity. This study aimed to test the hypothesis that SW elasticity is increased and SW dispersion slope is decreased in the right ventricle of monocrotaline (MCT)-induced pulmonary hypertension rats.

Methods: Rats were divided into MCT-induced pulmonary hypertension group (n = 10) and control group (n = 10). SW elasticity and SW dispersion slope were measured on excised hearts. Myocardial fibrosis was evaluated histologically.

Results: RV hypertrophy was observed in the MCT group. SW elasticity of right ventricle was higher in the MCT group than in the control group (3.5 ± 0.9 kPa vs. 2.5 ± 0.4 kPa, $p < 0.01$). SW dispersion slope of right ventricle was lower in the MCT group than in the control group (5.3 ± 1.7 m/s/kHz vs. 7.7 ± 1.5 m/s/kHz, $p < 0.01$). The fibrosis area of right ventricle was increased in MCT group compared with control group (18 ± 5% vs. 8 ± 3%, $p < 0.01$), and was positively related to SW elasticity and negatively related to SW dispersion slope.

Conclusions: Higher SW elasticity and lower SW dispersion slope were observed in the fibrotic myocardium of right ventricle in MCT-induced pulmonary hypertension rats. SWE may have

the potential to evaluate RV function by assessing myocardial characteristics.

Introduction

Right ventricular (RV) dysfunction has been associated with worse outcomes in patients with pulmonary hypertension or heart failure [1-4]. Fibrosis of RV myocardium leads to reduced RV function. The severity of fibrosis can be useful for assessing the disease severity, but it is difficult to evaluate non-invasively.

Shear wave elastography (SWE) is a novel ultrasound technique for assessing tissue characteristics based on shear wave (SW) propagation velocity, which estimates tissue elasticity and viscosity [5-7]. SW is generated by pushing pulses of ultrasound waves which deforms a part of the tissue, and SW speed is detected by tracking pulse. SWE can measure two parameters, such as SW elasticity and SW dispersion slope. SW elasticity, which is calculated by SW speed, is related to tissue hardness. Regarding SW dispersion slope, SW speed depends on the frequency of SWs in a visco-elastic tissue [8]. The gradient of SW speed, that is, the slope of SW speed versus SW frequency is changed in response to viscosity. Thus, SW dispersion slope can be used to estimate tissue viscosity.

SWE has been evaluated in several organs, such as the liver, breast, and thyroid [9-14]. In liver diseases, SW elasticity is correlated with the degree of fibrosis [9,10]. SW dispersion slope is associated with inflammation and necrosis [15-17]. In the field of heart diseases, a few studies reported that SWE could assess myocardial stiffness in animal models [18-20]. However,

the efficacy of SWE, including SW dispersion slope, has not been fully investigated. In particular, the relationship of SWE with myocardial characteristics remains unknown.

Monocrotaline (MCT)-induced pulmonary hypertension results in RV hypertrophy, leading to the progression of myocardial fibrosis. We hypothesized that SW elasticity is increased and SW dispersion slope is decreased in the right ventricle of pulmonary hypertension by reflecting the myocardial fibrosis. The aim of this study was to compare SWE of right ventricle between MCT-induced pulmonary hypertension rats and control rats, and to evaluate the relationship of SWE with the degree of myocardial fibrosis.

Methods

Animal models

Adult male Sprague-Dawley rats weighing 300-330 g (Charles River, Yokohama, Japan) were used for the experiments. Rats were housed under conditions of constant temperature (22℃) and humidity (60%), exposed to a 12-hour light/dark cycle, and offered tap water to drink. Rats were divided into two groups: MCT group (n = 10), which received subcutaneously 60 mg/kg MCT for 4 weeks to induce pulmonary hypertension, and control group (n = 10), which received 0.1 ml/kg saline. All surgery was performed under inhalation of 2% isoflurane anesthesia, and all efforts were made to minimize suffering. All animal protocols were approved and conducted in

accordance with the recommendations of the Okayama University Animal Care and Use Committee.

Echocardiography

Four weeks after the administration, transthoracic echocardiography was performed using Aplio ver. 6.0 with a 10-MHz sector probe (Canon Medical Systems, Otawara, Japan) under 2% isoflurane while lying in a left recumbent position. M-mode imaging was obtained in the parasternal short-axis view at the level of papillary muscles. RV end-diastolic, left ventricular (LV) end-diastolic, and LV end-systolic diameters were measured. Fractional shortening was calculated according to the formula.

Hemodynamic measurement

Rats were anesthetized, and right heart catheterization was performed on the beating hearts using high-fidelity 1.4F Millar catheters (Millar Instruments Inc., Houston, TX, USA). RV systolic pressure was measured with the PowerLab System using Chart 5.0 software (ADInstruments, Dunedin, New Zealand).

Shear wave elastography

SWE was analyzed by ex vivo experiment. The heart was rapidly excised and submerged in the Tyrode solution (136 mmol/L NaCl, 5.4 mmol/L KCl, 1.8 mmol/L $CaCl_2$, 0.53 mmol/L $MgC1_2$, 5.5 mmol/L HEPES, and 1% glucose, pH 7.4, 37℃) added to 20 mmol/L butanedione

monoxime, an inhibitor of actin-myosin interaction, and 10 μmol/L blebbistatin, a specific myosin II inhibitor. The ascending aorta was cannulated with an 18-gauge blunted needle connected to a retrograde perfusion system. The heart was perfused with the Tyrode solution added butanedione monoxime and blebbistatin to induce complete relaxation [21]. The heart was set in a water tank of agar phantom.

SWE was performed under a retrograde perfusion system using Aplio i900 with an 18-MHz linear probe (Canon Medical Systems) by two cardiologists. B-mode image was obtained in the parasternal long-axis view. A rectangular region of interest (ROI) was placed in RV wall. SW was generated by pushing pulse (Fig. 1A). After confirming proper SW propagation in "wave front" style display, two circular ROIs of 1-mm in diameter were placed in the images (Fig. 1B). SW speed was obtained based on the tissue Doppler technique. SW elasticity E was estimated by SW speed using the equation:

$$E = 3\rho c^2$$

where c is SW speed, and ρ is tissue density. Regarding the evaluation of SW dispersion slope, SW speed was transformed from time domain into frequency domain by Fourier transformation in order to estimate the phase change of SW at several frequencies. SW speed $c(\omega)$ at each frequency was calculated using the phase-difference method:

$$c(\omega) = \omega \, \Delta L/\Delta\varphi(\omega)$$

where $\Delta\varphi(\omega)$ is the phase change over the distance ΔL between two detected positions. SW dispersion slope, which is the gradient of SW speed, was calculated by the distribution of SW speed versus SW frequency [22]. SW elasticity and SW dispersion slope were measured automatically in the circular ROIs of RV wall. Each measurement was repeated five times.

Histological assessment

The hearts were fixed with 10% formalin, embedded in paraffin, and cut into 5-μm-thick sections. Sections were stained with hematoxylin and eosin for evaluating morphology, and with picrosirius red for detecting fibrosis. The widths of 30 individual cardiomyocytes were measured in regions containing the cellular nucleus. Interstitial fibrosis was measured using computer-assisted image analysis, and the percentage of fibrosis was calculated [23,24].

Statistical analysis

Data are presented as mean ± standard deviation for continuous variables. Variables were compared by Student *t* test and one-way analysis of variance. Relationships of SW elasticity and SW dispersion slope with the degree of myocardial fibrosis and the width of cardiomyocyte were assessed by Pearson's correlation coefficient. Inter- and intra-observer differences were analyzed. The measurements of SWE were evaluated by two blinded observers and by a single observer at two different times. Reliability was calculated by Pearson's

correlation coefficient. Variability was calculated as the percentage error of each measurement, and derived as the difference between the two measurements divided by the mean value. Statistical analysis was performed with JMP version 14.2 (SAS Institute Inc., Cary, NC, USA), and significance was defined as a value of $p < 0.05$.

Results

Baseline characteristics

Baseline characteristics are shown in Table 1. Body weight was significantly decreased in the MCT group compared with control group. RV weight and RV weight per LV weight were significantly increased in MCT group compared with control group. RV systolic pressure was higher in the MCT group than in control group. There were no significant differences in echocardiographic parameters between the two groups.

Shear wave elastography

Comparisons of SW elasticity and SW dispersion slope between the two groups are shown in Figure 2. SW elasticity of right ventricle was significantly higher in the MCT group than in control group (3.5 ± 0.9 kPa vs. 2.5 ± 0.4 kPa, $p < 0.01$). SW dispersion slope of right ventricle was significantly lower in the MCT group than in control group (5.3 ± 1.7 m/s/kHz vs. 7.7 ± 1.5 m/s/kHz, $p < 0.01$).

Histological evaluation

Histological findings of right ventricle stained with hematoxylin and eosin in the MCT group and control group are shown in Figure 3. The cardiomyocyte width was significantly increased in the MCT group compared with control group (9.9 ± 2.0 mm vs. 8.1 ± 0.9 mm, p = 0.03). Histological findings of right ventricle stained with picrosirius red in MCT group and control group are shown in Figure 4. The fibrosis area was significantly increased in the MCT group compared with control group (18 ± 5% vs. 8 ± 3%, $p < 0.01$). The fibrosis area was positively related to SW elasticity (r = 0.87, $p < 0.01$) and negatively related to SW dispersion slope (r = -0.53, p = 0.02) (Fig. 5A). The width of cardiomyocyte was positively related to SW elasticity (r = 0.63, $p < 0.01$) and negatively related to SW dispersion slope (r = -0.48, p = 0.04) (Fig. 5B). When the relationship between the fibrosis area and SW elasticity was corrected by the width of cardiomyocyte using multiple regression analysis, the fibrosis area remained to be significantly related to the increase of SW elasticity.

Reproducibility

There was a good reproducibility in the measurements of SW elasticity and SW dispersion slope between the two blinded observers (r = 0.99, $p < 0.01$), and for the intra-observer (r = 0.90, $p <$ 0.01). The inter- and intra-observer variabilities for SW elasticity and SW dispersion slope were 2.8% and 1.0%, respectively.

Discussion

The present study investigated the effectiveness of SWE for evaluating myocardial characteristics of right ventricle in MCT-induced pulmonary hypertension rats. The major findings of the present study were as follows. SW elasticity of right ventricle was increased and SW dispersion slope of right ventricle was decreased in MCT-induced pulmonary hypertension rats. SW elasticity was positively related to the fibrosis of right ventricle, and SW dispersion slope was negatively related. To our knowledge, this is the first study to assess the efficacy of SW elasticity and SW dispersion slope for assessing RV myocardial characteristics in pulmonary hypertension model.

RV function is an important factor for outcomes in patients with pulmonary hypertension or heart failure [25]. The non-invasive and repeatable method for evaluating RV myocardial characteristics is valuable for assessing the disease severity in clinical practice. SWE is a novel technique for characterizing tissues, such as the elasticity and viscosity. SWE has been used for assessing liver diseases [9,10,26-28]. Regarding the heart, SWE has been investigated in some animal models [18-20]. Pernot et al. reported that myocardial stiffness of left ventricle could be measured using SW imaging in ex vivo rat hearts [18]. They also reported that SW imaging evaluation of LV myocardial stiffness could differentiate between stiff,

noncompliant infarcted wall and softer wall containing stunned myocardium in beating ischemic hearts of ovine model [20]. In recent years, the feasibility of SW imaging has been shown in human subjects [29-31]. Villemain et al. reported that myocardial stiffness of left ventricle calculated by SW imaging was higher in patients with hypertrophic cardiomyopathy than in healthy volunteers [29]. Pislaru et al. reported that higher LV myocardial stiffness by elastography was observed in patients with cardiac amyloidosis [31]. However, the efficacy of SWE on heart diseases has not been well investigated. Although SWE can measure SW elasticity, which is related to the hardness of tissue, as well as SW dispersion slope, which reflects the viscosity of tissue [32], the assessments of SW dispersion slope are lacking. Furthermore, the relationship of SWE with histological evaluation has not been assessed in heart diseases.

The present study investigated SW elasticity and SW dispersion slope in the RV myocardium, including the relationships with tissue state. Higher SW elasticity and lower SW dispersion slope were observed in the RV myocardium of rats with MCT-induced pulmonary hypertension. These were related to the degree of fibrosis in the myocardium. MCT-induced pulmonary hypertension results in severe myocardial hypertrophy of right ventricle, causing the progression of myocardial fibrosis. Our findings suggest that SW elasticity and SW dispersion slope may have the possibility for evaluating the severity of fibrosis.

Clinical application

RV myocardial fibrosis causes RV dysfunction, leading to worse outcomes in patients with pulmonary hypertension. SWE, which can evaluate the degree of RV myocardial fibrosis, may be effective to assess the disease severity, such as the stage of RV dysfunction. Furthermore, therapeutic strategies for pulmonary hypertension are progressing [33,34]. Because SWE can detect the changes in myocardial characteristics, SWE may be useful as an indicator for therapeutic effects.

SWE is acquired by pushing pulse which deforms a part of the tissue. For the application of SWE in clinical practice, it is necessary to remove the influence of the beating of heart on SW propagation velocity, in order to accurately evaluate SWE. Recently, some studies have reported the feasibility of SW imaging under the beating hearts in human subjects [29]. Further development of this technique is needed, but the clinical application seems to be possible in the future.

Study limitations

There are some limitations in the present study. First, this study evaluated SWE in non-beating hearts. Since the rat's heart was beating at 350-400 beats per minutes, it was difficult to obtain SW imaging in the beating hearts. Thus, this study evaluated SWE in the completely relaxed myocardium under a retrograde perfusion system, which corresponds to the condition of the

end-diastolic phase. Second, a rectangular ROI placed in RV wall was larger, compared with RV wall thickness. This mismatch might affect our results. However, because SWE was measured in two circular ROIs of 1 mm in diameter on the image showing proper SW propagation, SWE values were considered to be appropriate in this study. Finally, SWE was measured in the long-axis view. SWE values might be different in the long- and short-axis views.

Conclusions

SW elasticity was higher and SW dispersion slope was lower in the right ventricle of MCT-induced pulmonary hypertension rats. SW elasticity and SW dispersion slope were related to the degree of myocardial fibrosis. Our findings suggest that SWE has the potential to provide valuable information for evaluating RV function by assessing myocardial characteristics.

Funding

This work was supported by Cannon Medical Systems.

Disclosure

The authors declare that there is no conflict of interest.

References

1. Meluzin J, Spinarova L, Hude P, Krejci J, Kincl V, Panovsky R, et al. Prognostic importance of various echocardiographic right ventricular functional parameters in patients with symptomatic heart failure. J Am Soc Echocardiogr 2005;18:435–44.
2. Juilliere Y, Barbier G, Feldmann L, Grentzinger A, Danchin N, Cherrier F. Additional predictive value of both left and right ventricular ejection fractions on long-term survival in idiopathic dilated cardiomyopathy. Eur Heart J 1997;18:276–80.
3. de Groote P, Millaire A, Foucher-Hossein C, Nugue O, Marchandise X, Ducloux G, et al. Right ventricular ejection fraction is an independent predictor of survival in patients with moderate heart failure. J Am Coll Cardiol 1998;32:948–54.
4. Noordegraaf AV, Westerhof BE, Westerhof N. The relationship between the right ventricle and its load in pulmonary hypertension. J Am Coll Cardiol 2017;69:236–43.
5. Sarvazyan AP, Rudenko OV, Swanson SD, Fowlkes JB, Emelianov SY. Shear wave elasticity imaging: a new ultrasonic technology of medical diagnostics. Ultrasound Med Biol 1998;24:1419-35.
6. Muller M, Gennisson JL, Deffieux T, Tanter M, Fink M. Quantitative viscoelasticity mapping of human liver using supersonic shear imaging: preliminary in vivo feasibility study. Ultrasound Med Biol 2009;35:219-29.

7. Chen S, Sanchez W, Callstrom MR, Gorman B, Lewis JT, Sanderson SO, et al. Assessment of liver viscoelasticity by using shear waves induced by ultrasound radiation force. Radiology 2013;266:964-70.

8. Chen S, Fatemi M, Greenleaf JF. Quantifying elasticity and viscosity from measurement of shear wave speed dispersion. J Acoust Soc Am 2004;115:2781-5.

9. Ferraioli G, Tinelli C, Dal Bello B, Zicchetti M, Filice G, Filice C. Accuracy of real-time shear wave elastography for assessing liver fibrosis in chronic hepatitis C: a pilot study. Hepatology 2012;56:2125-33.

10. Wong VW, Vergniol J, Wong GL, Foucher J, Chan HL, Le Bail B, et al. Diagnosis of fibrosis and cirrhosis using liver stiffness measurement in nonalcoholic fatty liver disease. Hepatology 2010;51:454-62.

11. Ogura I, Nakahara K, Sasaki Y, Sue M, Oda T. Usefulness of shear wave elastography in the diagnosis of oral and maxillofacial diseases. Imaging Sci Dent 2018;48:161-5.

12. Evans A, Whelehan P, Thomson K, McLean D, Brauer K, Purdie C, et al. Invasive breast cancer: relationship between shear-wave elastographic findings and histologic prognostic factors. Radiology 2012;263:673–7.

13. Liu Z, Jing H, Han X, Shao H, Sun YX, Wang QC, et al. Shear wave elastography combined with the thyroid imaging reporting and data system for malignancy risk

stratification in thyroid nodules. Oncotarget 2017;8:43406-16.

14. Honjo M, Moriyasu F, Sugimoto K, Oshiro H, Sakamaki K, Nasuya K, et al. Relationship between the liver tissue shear modulus and histopathologic findings analyzed by intraoperative shear wave elastography and digital microscopically assisted morphometry in patients with hepatocellular carcinoma. J Ultrasound Med 2014;33:61–71.

15. Sugimoto K, Moriyasu F, Oshiro H, Takeuchi H, Yoshimasu Y, Kasai Y, et al. Viscoelasticity measurement in rat livers using shear-wave US elastography. Ultrasound Med Biol 2018;44:2018-24.

16. Barry CT, Mills B, Hah Z, Mooney RA, Ryan CK, Rubens DJ, et al. Shear wave dispersion measures liver steatosis. Ultrasound Med Biol 2012;38:175-82.

17. Barry CT, Hah Z, Partin A, Mooney RA, Chuang KH, Augustine A, et al. Mouse liver dispersion for the diagnosis of early-stage fatty liver disease: a 70-sample study. Ultrasound Med Biol 2014;40:704-13.

18. Pernot M, Couade M, Mateo P, Crozatier B, Fischmeister R, Tanter M. Real-time assessment of myocardial contractility using shear wave imaging. J Am Coll Cardiol 2011;58:65–72.

19. Vos HJ, van Dalen BM, Heinonen I, Bosch JG, Sorop O, Duncker DJ, et al. Cardiac shear wave velocity detection in the porcine heart. Ultrasound Med Biol 2017;43:753–64.

20. Pernot M, Lee WN, Bel A, Mateo P, Couade M, Tanter M, et al. Shear wave imaging of passive diastolic myocardial stiffness: stunned versus infarcted myocardium. JACC Cardiovasc Imaging 2016;9:1023–30.

21. Sumita-Yoshikawa W, Nakamura K, Miura D, Shimizu J, Hashimoto K, Kataoka N, et al. Increased passive stiffness of cardiomyocytes in the transverse direction and residual actin and myosin cross-bridge formation in hypertrophied rat hearts induced by chronic β-adrenergic stimulation. Circ J 2013;77:741-8.

22. Sugimoto K, Moriyasu F, Oshiro H, Takeuchi H, Abe M, Yoshimasu Y, et al. The role of multiparametric US of the liver for the evaluation of nonalcoholic steatohepatitis. Radiology 2020;296:532–40.

23. Gallego B, Arevalo MA, Flores O, Lopez-Novoa JM, Perez-Barriocanal F. Renal fibrosis in diabetic and aortic-constricted hypertensive rats. Am J Physiol Regul Integr Comp Physiol 2001;280:R1823-9.

24. Takemoto M, Egashira K, Tomita H, Usui M, Okamoto H, Kitabatake A, et al. Chronic angiotensin-converting enzyme inhibition and angiotensin II type 1 receptor blockade: effects on cardiovascular remodeling in rats induced by the long-term blockade of nitric oxide synthesis. Hypertension 1997;30:1621-7.

25. Amano M, Izumi C, Baba M, Abe R, Matsutani H, Inao T, et al. Progression of right

ventricular dysfunction and predictors of mortality in patients with idiopathic interstitial pneumonias. J Cardiol 2020;75:242-9.

26. Tada T, Kumada T, Toyoda H, Ito T, Sone Y, Okuda S, et al. Utility of real-time shear wave elastography for assessing liver fibrosis in patients with chronic hepatitis C infection without cirrhosis: comparison of liver fibrosis indices. Hepatol Res 2015;45:E122-9.

27. Sasso M, Beaugrand M, de Ledinghen V, Douvin C, Marcellin P, Poupon R, et al. Controlled attenuation parameter (CAP): a novel VCTE™ guided ultrasonic attenuation measurement for the evaluation of hepatic steatosis: preliminary study and validation in a cohort of patients with chronic liver disease from various causes. Ultrasound Med Biol 2010;36:1825-35.

28. Parker KJ, Partin A, Rubens DJ. What do we know about shear wave dispersion in normal and steatotic livers? Ultrasound Med Biol 2015;41:1481-7.

29. Villemain O, Correia M, Mousseaux E, Baranger J, Zarka S, Podetti I, et al. Myocardial stiffness evaluation using noninvasive shear wave imaging in healthy and hypertrophic cardiomyopathic adults. JACC Cardiovasc Imaging 2019;12:1135-45.

30. Song P, Bi X, Mellema DC, Manduca A, Urban MW, Greenleaf JF, et al. Quantitative assessment of left ventricular diastolic stiffness using cardiac shear wave elastography: a pilot study. J Ultrasound Med 2016;35:1419-27.

31. Pislaru C, Lonescu F, Alashry M, Petrescu I, Pellikka PA, Grogan H, et al. Myocardial stiffness by intrinsic cardiac elastography in patients with amyloidosis: comparison with chamber stiffness and global longitudinal strain. J Am Soc Echocardiogr 2019;32:958-68.

32. Deffieux T, Montaldo G, Tanter M, Fink M. Shear wave spectroscopy for in vivo quantification of human soft tissues visco-elasticity. IEEE Trans Med Imaging 2009;28:313-22.

33. Akagi S, Matsubara H, Nakamura K, Ito H. Modern treatment to reduce pulmonary arterial pressure in pulmonary arterial hypertension. J Cardiol 2018;72:466-72.

34. Minatsuki S, Kiyosue A, Kodera S, Hara T, Saito A, Maki H, et al. Effectiveness of balloon pulmonary angioplasty in patients with inoperable chronic thromboembolic pulmonary hypertension despite having lesion types suitable for surgical treatment. J Cardiol 2020;75:182-8.

Figure legends

Figure 1 Shear wave elastography. (A) SW is generated by pushing pulse of ultrasound wave. (B) SW propagation images in MCT group and control group are shown. Two circular ROIs were placed in the images. SW elasticity and SW dispersion slope were measured.

Ao, aorta; LV, left ventricle; MCT, monocrotaline; ROI, region of interest; RV, right ventricle; SW, shear wave.

Figure 2 Comparison of SW elasticity and SW dispersion slope. SW elasticity and SW dispersion slope of right ventricle was compared between MCT group (n = 10) and control group (n = 10).

MCT, monocrotaline; SW, shear wave.

Figure 3 Cardiomyocyte width. (A) Histological findings of right ventricle stained with hematoxylin and eosin. A digital microscopic image was high-power view. Scale bar indicates 50μm. (B) The cardiomyocyte width was compared between MCT group (n = 10) and control group (n = 10).

MCT, monocrotaline.

Figure 4 Myocardial fibrosis. (A) Histological findings of right ventricle stained with picrosirius red. Fibrosis was shown as red color. A digital microscopic image was high-power view. Scale bar indicates 50μm. (B) The fibrosis area was compared between MCT group (n = 10) and control group (n = 10).

MCT, monocrotaline.

Figure 5 Relationships of SW elasticity and SW dispersion slope with myocardial fibrosis and cardiomyocyte width. (A) Relationships of SWE elasticity (left) and SWE dispersion slope (right) with the fibrosis area in MCT group and control group (n = 20). (B) Relationships of SWE elasticity (left) and SWE dispersion slope (right) with the width of cardiomyocyte in MCT group and control group (n = 20).

MCT, monocrotaline; SW, shear wave; SWE, shear wave elastography.

Highlights

- Shear wave elastography (SWE) is a novel technique for assessing tissues.
- Shear wave (SW) elasticity of right ventricle was higher in pulmonary hypertension.
- SW dispersion slope of right ventricle was lower in pulmonary hypertension.
- SW elasticity and dispersion slope were related to myocardial fibrosis.
- SWE has the potential to evaluate myocardial characteristics.

figure 1A

figure 1B

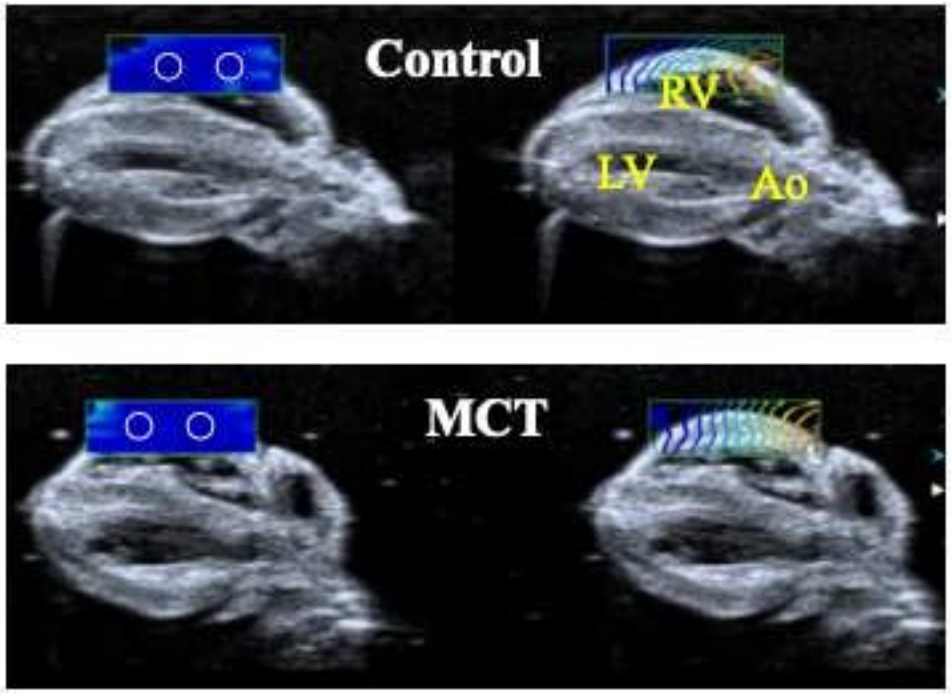

figure 2

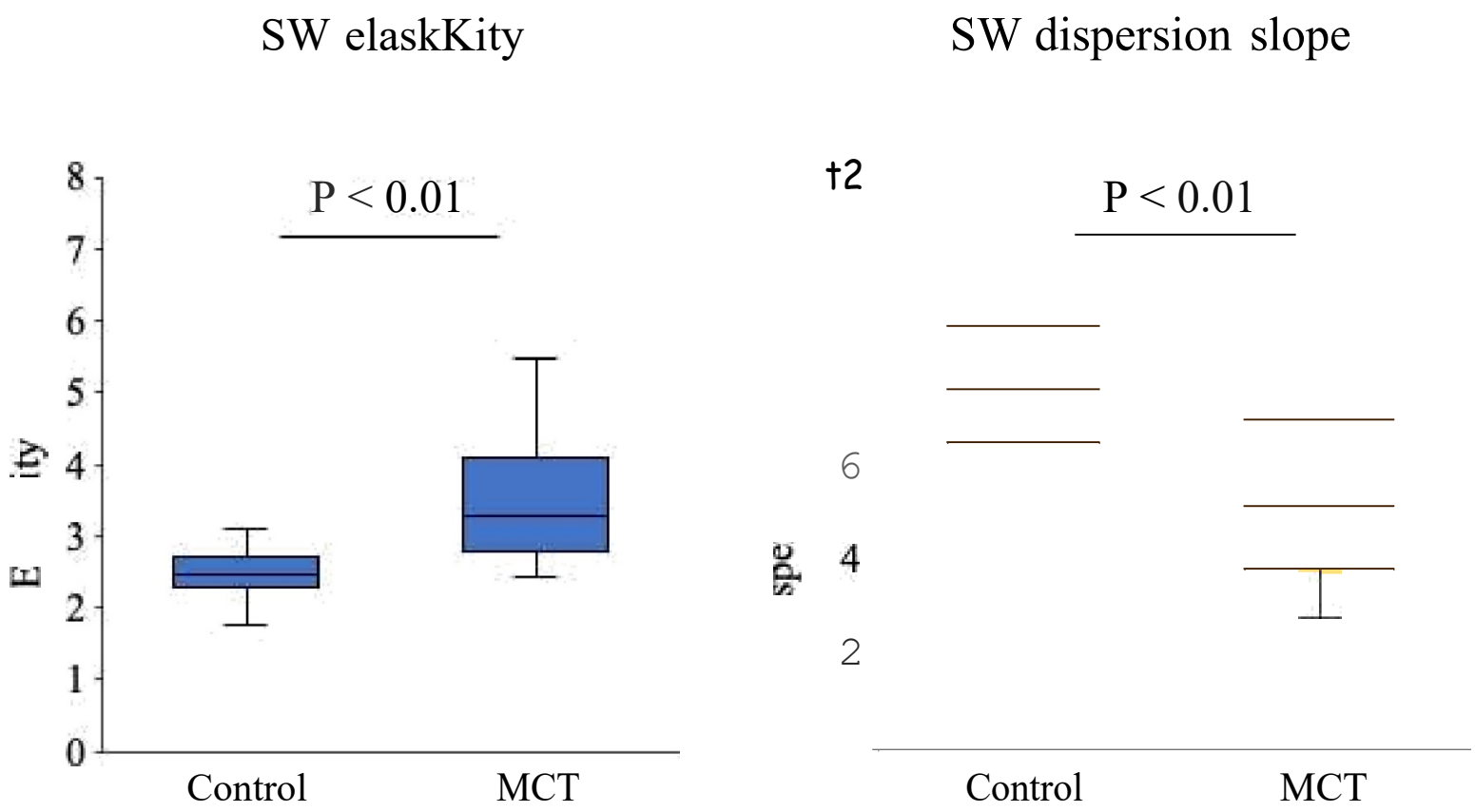
SW elaskKity
P < 0.01
8
7
6
5
4
3
2
1
0
ity
E
Control
MCT
SW dispersion slope
P < 0.01
t2
6
4
2
spe
Control
MCT

figure 3A

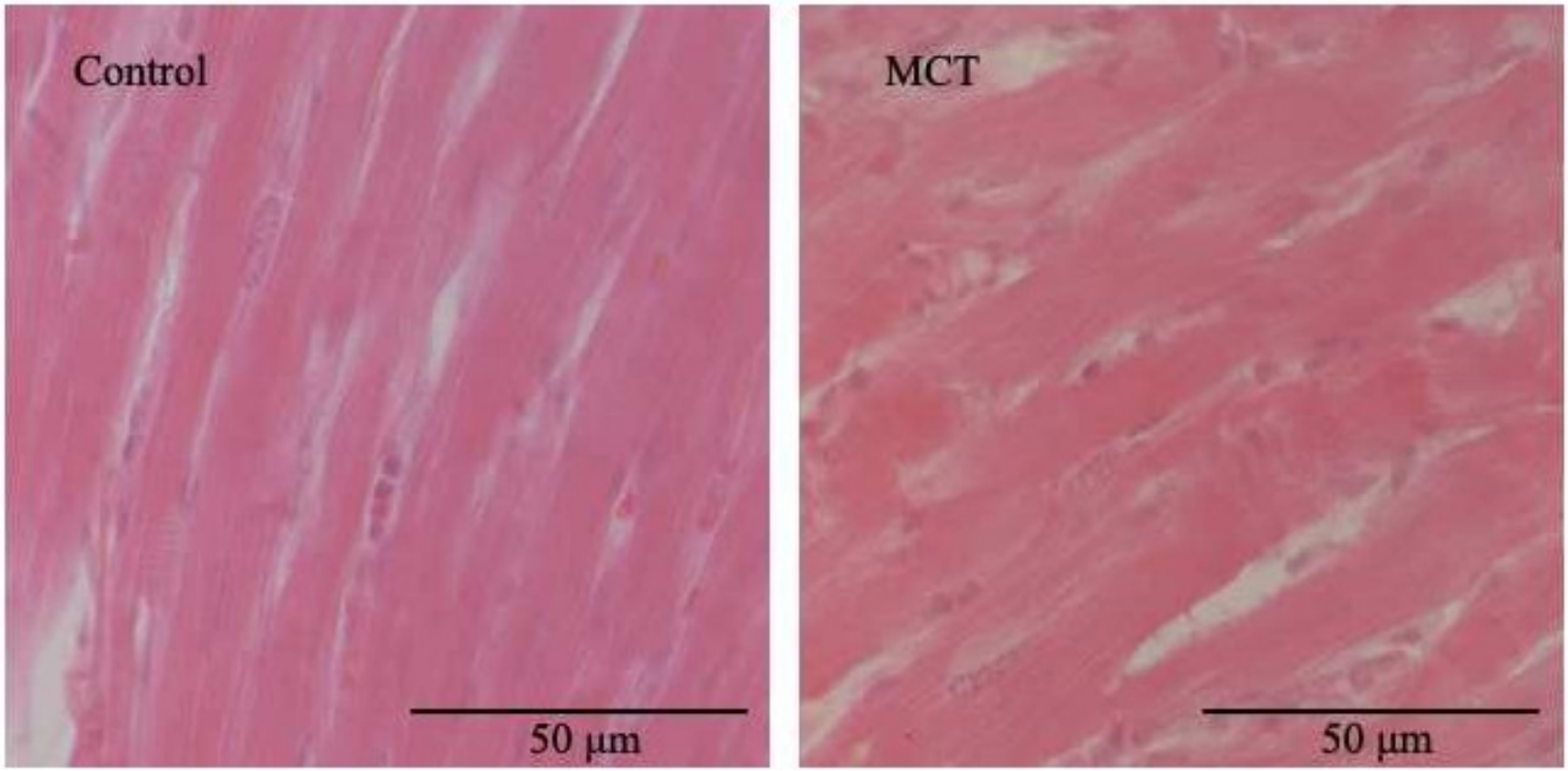

figure 3B

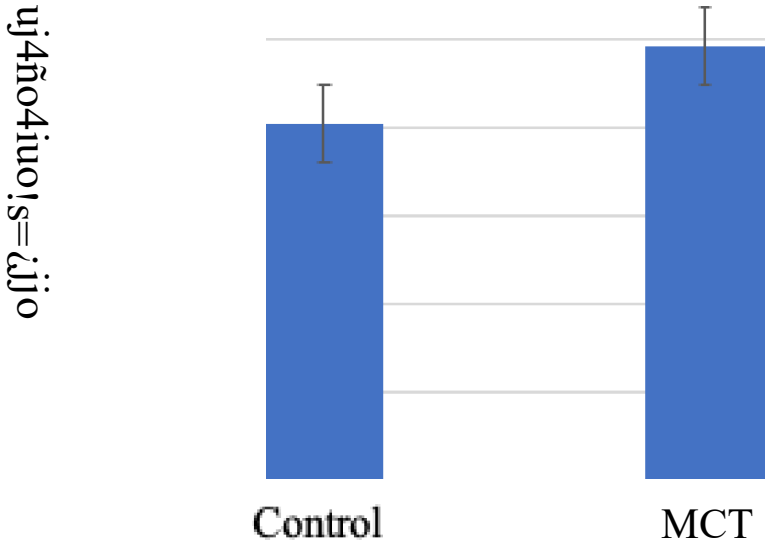

figure 4A

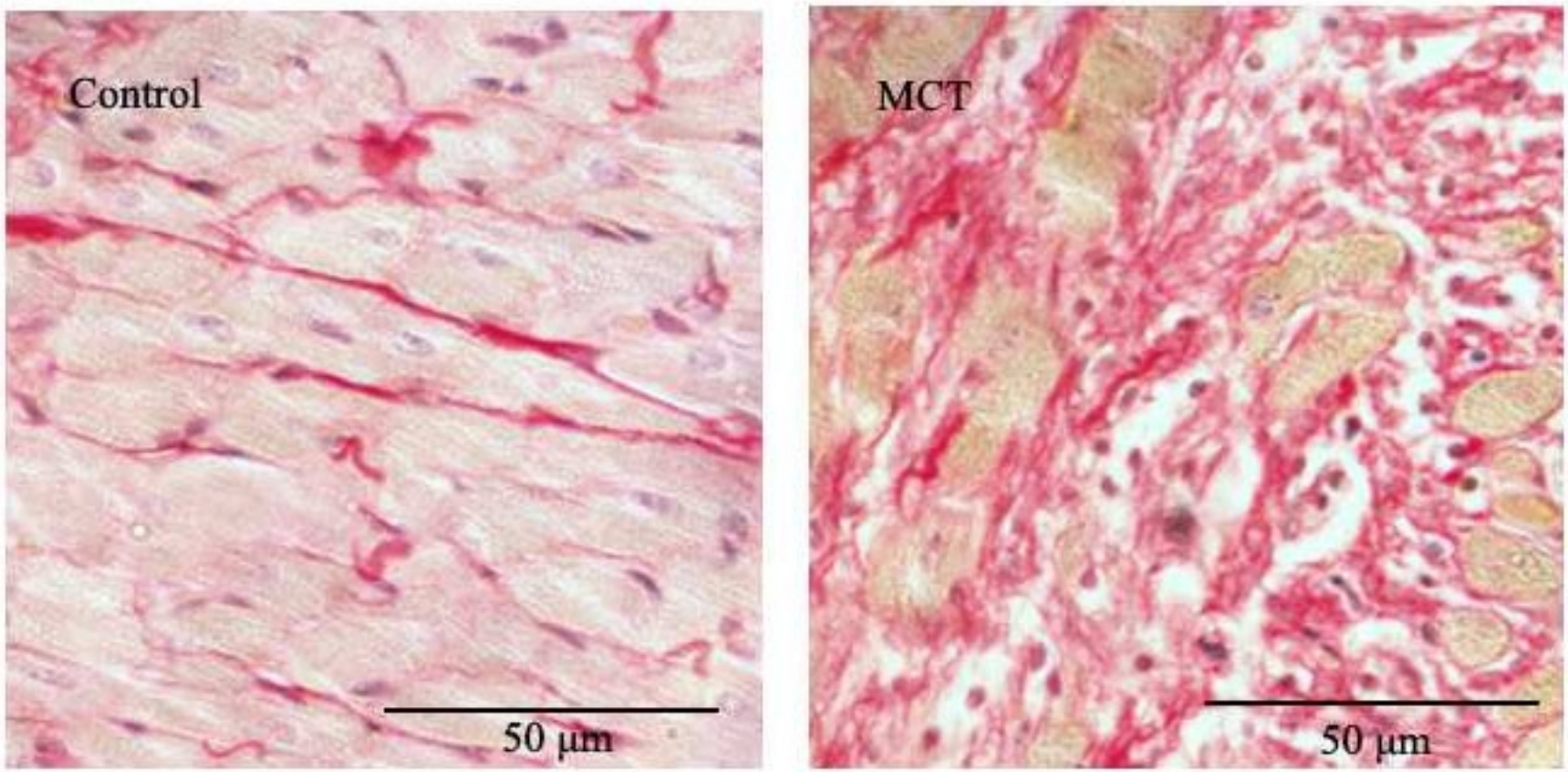

figure 4B

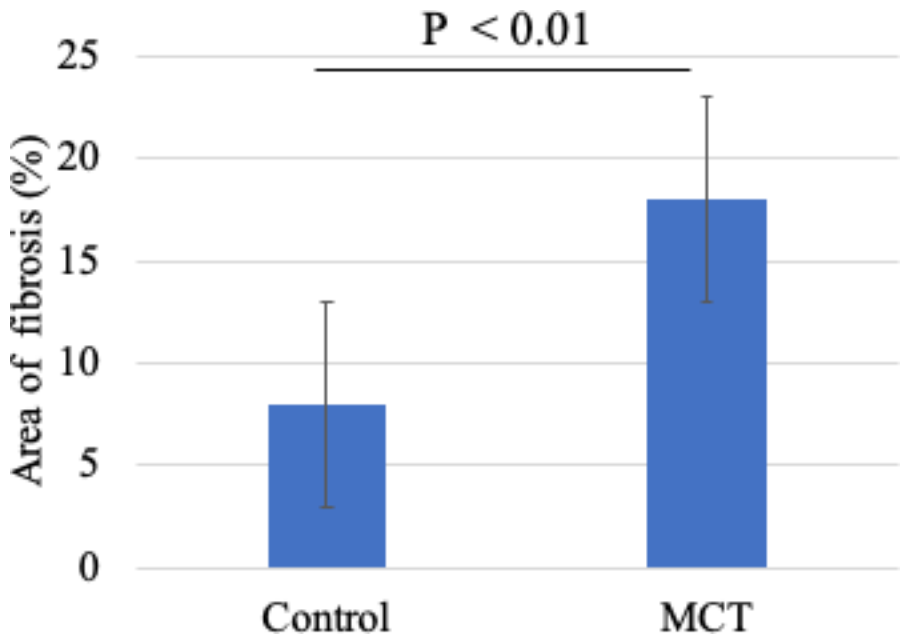

Figure 5A

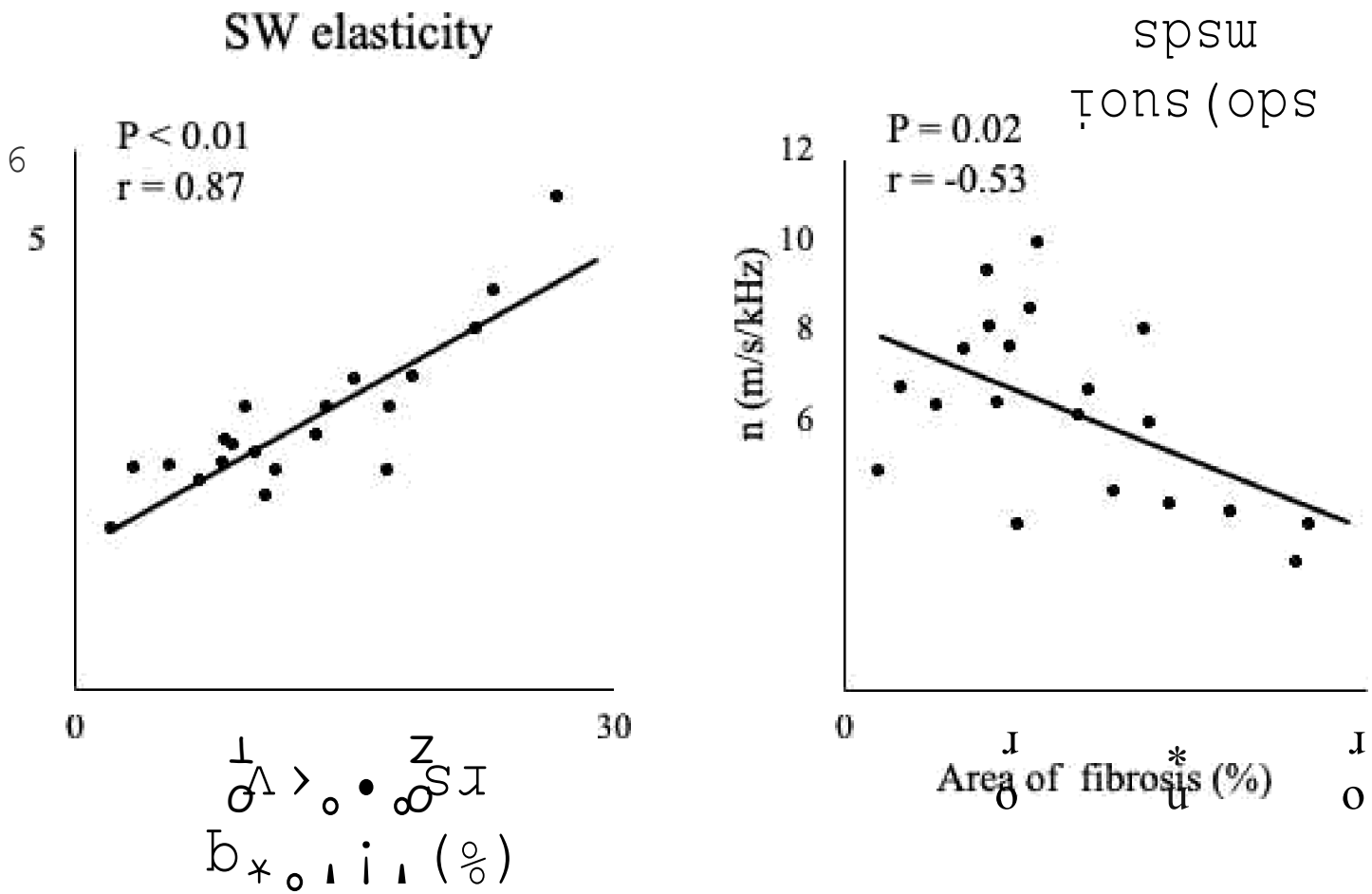
SW elasticity
P < 0.01
r = 0.87
6
5
0
30
spsw
ţons(ops
P = 0.02
r = -0.53
12
10
8
6
n (m/s/kHz)
0
Area of fibrosis (%)

Figure 5B

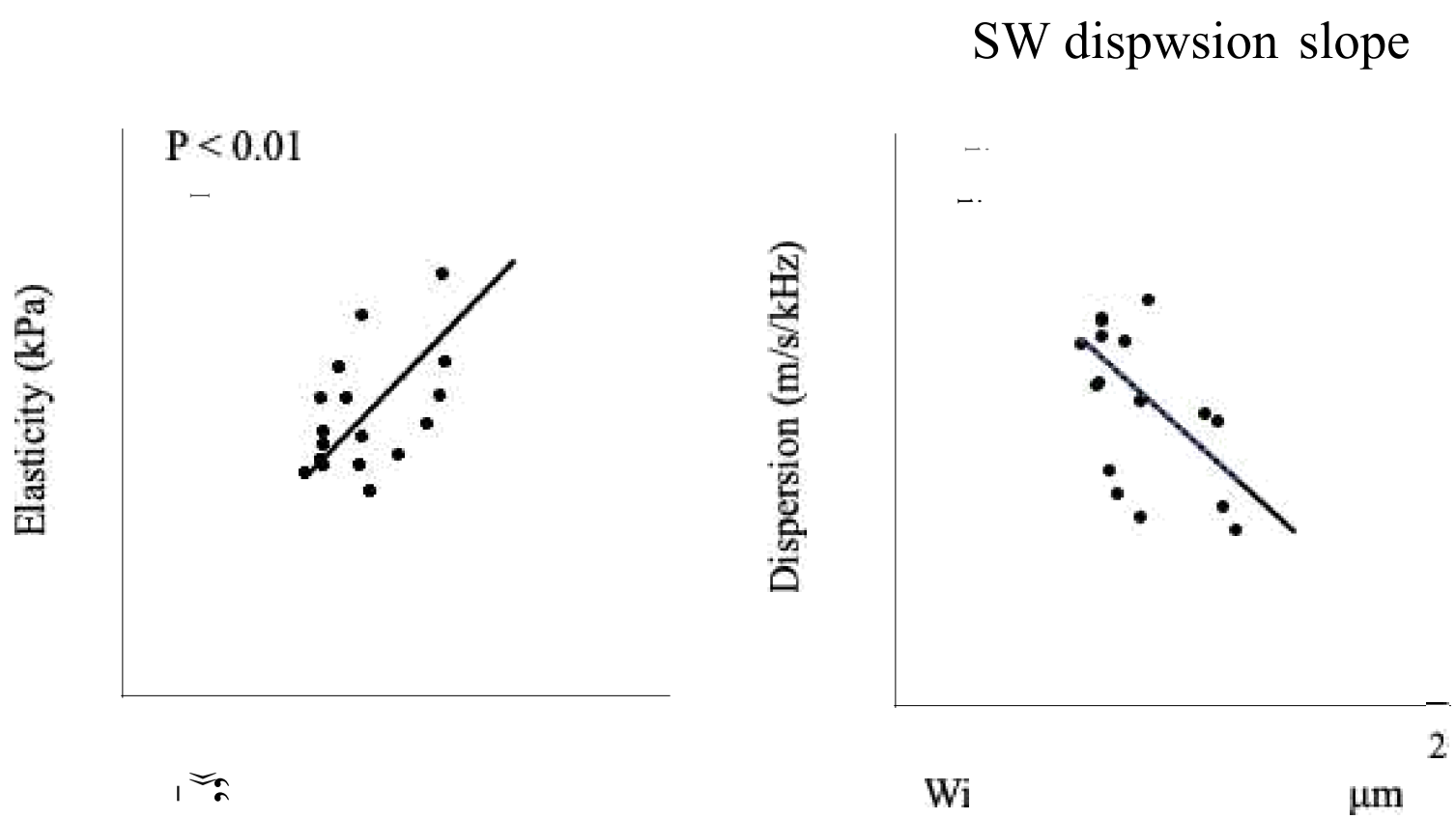
SW dispwsion slope
P < 0.01
Elasticity (kPa)
Dispersion (m/s/kHz)
Wi
µm
2

Table

Table 1 Baseline Characteristics.

Variables	MCT group (n = 10)	Control group (n = 10)	*p*
Body weight (g)	402 ± 27	443 ± 15	< 0.01
Heart rate (bpm)	291 ± 58	313 ± 25	0.57
RV weight (g)	0.5 ± 0.1	0.3 ± 0.1	< 0.01
LV weight (g)	1.1 ± 0.2	1.1 ± 0.1	0.69
RV weight / LV weight	0.5 ± 0.1	0.2 ± 0.1	< 0.01
Echocardiography			
RV end-diastolic diameter (mm)	1.6 ± 1.6	0.7 ± 0.4	0.14
LV end-diastolic diameter (mm)	8.0 ± 0.9	7.3 ± 1.0	0.14
LV end-systolic diameter (mm)	4.7 ± 0.9	4.2 ± 0.8	0.22
Fractional shortening (%)	42 ± 8	43 ± 5	0.65
Catheterization			
RV systolic pressure (mmHg)	55 ± 6	25 ± 3	< 0.01

Data are presented as mean ± standard deviation.

MCT, monocrotaline; RV, right ventricular; LV, left ventricular.